ELSEVIER

Biophysical Chemistry 71 (1998) 173–184

Biophysical Chemistry

Monte Carlo studies on potentiometric titration of poly(glutamic acid)

Takuhiro Nishio *

Department of Physics, Hamamatsu University School of Medicine, Hamamatsu 431-3192, Japan

Received 17 September 1997; revised 8 December 1997; accepted 25 December 1997

Abstract

The potentiometric titration of poly(glutamic acid) with special attention to its helix–coil transition is investigated in terms of the previously developed Monte Carlo method. The simulations of the potentiometric titration are carried out for helical and coiled form of the peptide, separately. A cylindrical rod with spherical ionizable groups is adopted as each conformational model of poly(glutamic acid) molecule. A spherical charge with a hard core potential is assumed as a mobile hydrated ion. The helix–coil transition curves are analyzed by the Zimm–Bragg theory. A satisfactory agreement is achieved for the titration curves with the experimental data in most cases. The significance and the limitations of the simulation method are discussed.

Keywords: Potentiometric titration; Poly(glutamic acid) (PGA); Monte Carlo simulation; Linear polyelectrolyte; Helix–coil transition; Zimm–Bragg theory

1. Introduction

Poly(glutamic acid) (PGA) is a typical synthetic homopolypeptide that undergoes the helix-to-coil transition induced by ionization [1]. Numerous experimental studies have been carried out for the potentiometric titration of this weak polyacid. The helix–coil transition has been analyzed with the theoretical framework founded on statistical mechanics [2,3]. Recent experimental measurements of the α-helix propensities of amino acids have raised a renewed interest in the α-helix formation studies [4–6].

In the polyelectrolyte study, various theoretical treatments have been applied to the potentiometric titrations of the PGA helix and coil. From a point of view of the protein research, the helix formation of the polypeptide has been investigated in detail. A sufficient quantitative description of the titration behavior is, however, not yet achieved by adopting the reasonable molecular dimensions.

Here, the object is to reproduce the titration curve of PGA accompanying the helix–coil transition with the previously developed Monte Carlo (MC) method [7]. The MC simulations on the potentiometric titration are performed for PGA in α-helical and extended coil forms. Fittings are attempted to the helix–coil transition curves using a classical theoretical treatment by Zimm and Bragg [8]. Comparisons are examined between the results of the MC simulation and the typical data in the literature.

* Corresponding author.

0301-4622/98/$19.00
PII S0301-4622(98)00094-5

First, the models are built for α-helix and extended coil of PGA. Each MC result is compared with the data for α-helix of D-PGA and for coil of DL-PGA, respectively. Next, the titration curve for the helical and coiled L-PGA is calculated, and the helix–coil transition is fitted by the Zimm–Bragg theory. Dependence on the polymer concentration, ionic strength and temperature are examined precisely. The remaining problems, as well as the comparisons with the experiments, are discussed.

2. Method and models

2.1. Algorithm of the MC simulation in cylindrical cell system

The details of the computational method were described in the previous papers [7,9]. Only its essence is noted here.

An aqueous PGA solution is treated as an isolated cylindrical cell system. A rigid rod of the modeled PGA molecule is centered in the objective cell. The N^p carboxyl groups are attached to the PGA backbone rod, whose length is equal to the height of the cell, H. The mean axial distance per group is given by $b = H/N^p$. The cell radius, R, is determined by the concentration of the carboxyl group in the solution C^p. A neutral un-ionized carboxyl group, with own intrinsic dissociation constant K_0, can dissociate into a mobile counterion and an ionized group by the ionization. The N^s cations and the same number of anions from the 1:1 salt are distributed in the cell. The cell end effect is eliminated by connecting the long external cells. These cell dimensions are determined on account of the accuracy and the computational time for the calculation.

The MC trial in the iterative loop of the simulation consists of four processes: (1) ionization of an un-ionized group, (2) deionization of an ionized group, (3) movement of a counterion, and (4) movement of an ion from added salt. If a group is in the un-ionized state, process (1) is tried or nothing is done. If the group is ionized, (2) or (3) is chosen in a given probability. Trial process (4) is added to the simulation in the case of salt solution.

The energy change with ionization is determined by the difference of the aqueous pH and $\mathrm{p}K_0$, the negative logarithm of K_0. The intrinsic $\mathrm{p}K_0$ value of the carboxyl group is defined in the infinitely dilute solution without added salt. Therefore, the contribution of the electric interaction is not considered, except for the self-energy by definition.

The average degree of ionization, α, and other average values are obtained in an iterative loop after the convergence is fulfilled. The negative logarithm of apparent dissociation constant, $\mathrm{p}K_\mathrm{a}$ and the electrostatic term of $\mathrm{p}K_\mathrm{a}$, $\Delta\mathrm{p}K$, is related to a given solution pH, $\mathrm{p}K_0$, and α, expressed by the following equation,

$$\Delta\mathrm{p}K = \mathrm{p}K_\mathrm{a} - \mathrm{p}K_0 = \mathrm{pH} - \mathrm{p}K_0 + \log\left[(1-\alpha)/\alpha\right] \tag{1}$$

The $\Delta\mathrm{p}K$ is evaluated using a given $\mathrm{pH}-\mathrm{p}K_0$ value and an average degree of ionization, α. The $\mathrm{p}K_\mathrm{a}$ value is determined by adding a suitable $\mathrm{p}K_0$ to the $\Delta\mathrm{p}K$. Then, the calculated titration curve can be compared with the experimental data.

2.2. Molecular models for α-helix and extended coil

The present work is planned to compare the MC results with the several titration data of the PGA in the 1:1 salt solution. The molecular model of the helix or that of the extended coil is treated as a rigid impenetrable cylinder with the spherical ionizable groups, similar to the previous study for (carboxymethyl)cellulose (CMC) [9]. A counterion from the ionized group, as well as an ion from the salt is also treated as a charged sphere with a hard core potential. The energy between two charged species, labeled as i and j, is defined as the Coulombic interaction in uniform dielectric medium with the hard core repulsion, as follows:

$$u_{ij} = \begin{cases} \dfrac{e^2}{4\pi\varepsilon_0 D}\dfrac{z_i z_j}{|\boldsymbol{r}_i - \boldsymbol{r}_j|} & |\boldsymbol{r}_i - \boldsymbol{r}_j| > \sigma_i + \sigma_j \\ \infty & |\boldsymbol{r}_i - \boldsymbol{r}_j| \le \sigma_i + \sigma_j \end{cases} \tag{2}$$

where z, r and σ with subscript i or j denote the valence, the position and the radius of each species, respectively; e, the elementary protonic charge; ε_0, the permittivity of the vacuum; and D, the relative dielectric constant of the solvent water. The radius of the mobile ions, σ_m, 2.0 Å, is adopted for both conformations in most cases. The same value, σ_m, is

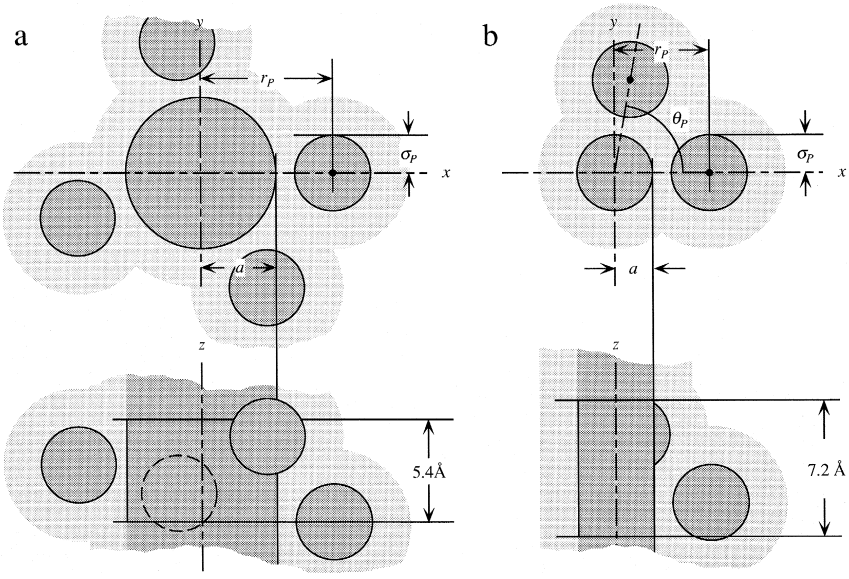

Fig. 1. Molecular models of the α-helical PGA (a) and extended DL-PGA coil (b). Top view and the side view of one helical unit are presented for each conformation with the volume from which the centers of the mobile ions are excluded. Here, θ^p is assumed to be 80° for DL-PGA coil (b). On the other hand, θ^p is assumed to be 180° in the case of L-PGA coil. See text.

adopted as the radius of ionizable group to facilitate the analysis.

The standard dimension of the conformations is used at each molecular model here. The details are described on each model and on the comparison with data as follows.

2.2.1. α-Helix

The simulation is designed to compare the MC results with the titration data of the left-handed helix of poly(D-glutamic acid) in NaCl solution by Muroga et al. [10]. The dimensions of the α-helical form are shown in Fig. 1a (here, no essential difference exists between L-PGA and D-PGA). The radius of the rod, a, is 4.0 Å, and the distance of the center of each ionizable group from the rod axis origin, r^p is 7.0 Å (equal to backbone radius 2.5 Å plus side chain length 4.5 Å). The helical order is 5.4 Å/turn (= 3.6 groups/turn × 1.5 Å/group). In the model, mean axial distance per group, b, is 1.5 Å.

Table 1
Parameters of the objective cell for the MC simulation of α-helical PGA

Label	C^p (N)	C^s (M)	N^p	N^s	R (Å)	H (Å)	MCS	Symbol
A-a1	0.003	0.01	90	300	342.723	135.0	2000	Inversed triangle
A-b2	0.005	0.01	72	144	265.472	108.0	4000	Square
B-b2	0.005	0.02	72	288	265.472	108.0	3000	Square
B-c2	0.01	0.02	72	144	187.717	108.0	4000	Circle
C-c3	0.01	0.05	54	270	187.717	81.0	2000	Circle
C-d4	0.02	0.05	36	90	132.736	54.0	5000	Diamond
D-d4	0.02	0.1	36	180	132.736	54.0	4000	Diamond
D-e4	0.03	0.1	36	120	108.379	54.0	5000	Triangle
E-e4	0.03	0.2	36	240	108.379	54.0	3000	Triangle

MCS is the number of the Monte Carlo step per group for a titration point.
Symbols in the rightmost column are used in Fig. 2.

The polymer concentration, C^p, of their experiments was in the range 0.001–0.003 N. In the simulation, the range 0.003–0.03 N is applied to avoid the long computational time. The dependence on the polymer concentration is checked by two calculations in the different C^p for each titration curve. The cell sizes and other parameters are shown in Table 1.

2.2.2. Extended coil

The coiled state of the polypeptide is assumed as an extended (not random) coil. The extended coil of PGA is considered to compare the MC results with the titration data of poly(DL-glutamic acid) in NaCl solution measured by Olander and Holtzer [11]. This synthetic polypeptide remains in a coil conformation over the entire titration range. The extended peptide chain is adopted in the simulation as a molecular model. In the case, a, r^p and b are 2.0 Å, 5.0 (= 0.5 + 4.5) Å, and 3.6 Å, respectively. The length per its repetition unit is 7.2 Å/unit (= 2 groups/unit × 3.6 Å/group). The neighbor groups are located with the width of angle, θ^p, 80° on the rod surface (Fig. 1b).

The C^p value of the experiments was not described explicitly in their paper. It seems that C^p was in the range 0.012–0.02 N guessed from the values in the other experiments. In the MC simulation, the values in the range 0.005–0.02 N is applied. The cell sizes and other parameters are listed in Table 2.

2.3. Analysis of the helix–coil transition

The fitting of the helix–coil transition is performed for the titration curves of the L-PGA molecule. Its helix–coil transition is analyzed with the well-known Zimm–Bragg theory, which is based on the Ising model [2,8]. To analyze the energetic properties, the following procedures are carried out for the helix–coil transitions [12].

2.3.1. MC simulations for helical and coiled forms

First, the MC simulations are attempted for the helical form and for the extended coil form of PGA separately. Molecular models used here are the same as those in the above simulations. An ionizable group on the coiled L-PGA, however, is arranged alternately in the opposite position with respect to the main chain rod ($\theta^p = 180°$ in Fig. 1b). The curves of (pH–pK_0) versus α^h and α^c are obtained by the separated simulations for the helical and coiled models, where α^h and α^c are the degree of ionization in the helix and coil portion, respectively.

2.3.2. Evaluation of equilibrium constant

The microscopic equilibrium between the states of the helix and coil is considered in a polypeptide, for example,

$$\cdots hhhcc \cdots \leftrightarrow \cdots hhccc \cdots \quad (3)$$

where h and c denote the helical and coiled state of the residue, respectively. The equilibrium constant of the helix–coil transition (growth parameter), s, is divided into the intrinsic term, s_0, and the electrostatic contribution, s', as the following relationships [12]:

$$s = s_0 s'$$

$$s_0 = \frac{h_0}{c_0} \quad (4)$$

where h_0 and c_0 are the partition functions per

Table 2
Parameters of the objective cell for the MC simulation of extended coil PGA

Label	C^p (N)	C^s (M)	N^p	N^s	R (Å)	H (Å)	MCS	Symbol
F-h6	0.005	0.01	40	80	171.362	144.0	5000	Inversed triangle
F-f6	0.01	0.01	40	40	121.171	144.0	5000	Square
F-g6	0.02	0.01	40	20	85.681	144.0	10 000	Circle
G-f7	0.01	0.05	30	150	121.171	108.0	5000	Square
G-g6	0.02	0.05	40	100	85.681	144.0	5000	Circle
H-f8	0.01	0.1	20	200	121.171	72.0	5000	Square
H-g7	0.02	0.1	30	150	85.681	108.0	5000	Circle
I-g9	0.02	0.4	12	240	85.681	43.2	5000	Circle

Symbols in the rightmost column are used in Fig. 3.

residue of the pure helical and pure coiled forms in the uncharged states, respectively. The standard free energy change of the helix–coil transition per residue Δg°_{hc} is calculated from s_0 for a sufficiently long peptide by the following equation:

$$\Delta g^{\circ}_{hc} = k_B T \ln s_0 \quad (5)$$

where k_B is the Boltzmann constant and T, the absolute temperature. The value s_0 has a relation with the pH vs. α curves of coiled and helical form [13],

$$\ln s_0 = \ln(10) \int_{pH_0}^{pH_m} (\alpha_c - \alpha_h)\, d\mathrm{pH} \quad (6)$$

where pH_m is pH at the midpoint of the transition, and pH_0 is the value of pH corresponding to $\alpha_h = \alpha_c$. On the other hand, the value s' is evaluated by the following relation:

$$\ln s' = -\int_{\lambda(0)}^{\lambda(\alpha)} (\alpha_c - \alpha_h)\, d\ln\lambda \quad (7)$$

where the variable λ plays the role of the reciprocal of the absolute activity of the hydrogen ion [2],

$$\ln\lambda = \ln(10)(\mathrm{pH} - \mathrm{p}K_0) \quad (8)$$

Rigorously speaking, the addition of a small constant term relating to the solution conditions is necessary in the right-hand side of Eq. (8). However, the omission of the term does not change the practical integrations. Then, the following equation for the numerical integration,

$$\ln s' = -\ln(10) \int_{pH_0}^{pH} (\alpha_c - \alpha_h)\, d\mathrm{pH}' \quad (9)$$

is obtained. To evaluate s' from the MC data, the numerical integration, Eq. (9), is performed using appropriate fitting functions for $(\mathrm{pH}-\mathrm{p}K_0)$ vs. α_h and α_c.

2.3.3. Fitting of the transition curves

The fraction of the helical state of a long peptide, θ, is expressed as the following function of s and σ [14],

$$\theta = \frac{1}{2}\left\{1 + \frac{s-1}{\left[(s-1)^2 + 4s\sigma\right]^{1/2}}\right\} \quad (10)$$

where σ is the nucleation parameter characterizing the initiation of a helical portion. The parameter σ determines the 'sharpness' of the transition. By giving s_0 and σ, the fraction of the helical state can be determined by s'. When the helical content is θ, the average degree of ionization is described on the way of transition, as follows:

$$\alpha = \theta\alpha_h + (1-\theta)\alpha_c \quad (11)$$

$\Delta \mathrm{p}K$ is calculated from this α value by Eq. (1). In the relation, the end effect of each portion is ignored. Then, the transition curve is compared with the experimental results when the common $\mathrm{p}K_0$ value is assumed.

Table 3
Parameters of the objective cell of the helical and coiled PGA to investigate the polymer concentration dependence compared with the data by Nitta et al.

Label	C_p (N)	C_s (M)	N_p	N_s	Helix		Coil		MCS	Symbol
					R (Å)	H (Å)	R (Å)	H (Å)		
r-1	0.006498	0.05	72	554	232.867	108.0	150.315	259.2	2000	Square
r-2	0.01319	0.05	72	273	163.469	108.0	105.518	259.2	3000	Circle
r-3	0.02769	0.05	72	130	112.804	108.0	72.815	259.2	5000	Square
q-1	0.006506	0.005	108	83	232.727	162.0	150.224	388.8	5000	Square
q-2	0.01200	0.005	108	45	171.362	162.0	110.613	388.8	5000	Circle
q-3	0.01929	0.005	108	28	135.172	162.0	87.253	388.8	5000	Square
q-4	0.03600	0.005	108	15	98.936	162.0	63.863	388.8	5000	Circle

Upper three rows are for low C^p cases (Fig. 4a) and lower four rows are for high C^p cases (Fig. 4b).
Symbols in the rightmost column are used in Fig. 4.

Table 4
Parameters of the objective cell of the helical and coiled PGA to compare with the experimental data by McDiarmid and Doty

	Label	C^p (N)	C^s (M)	N^p	N^s	R (Å)	H (Å)	MCS
Helix	K-ka	0.0004	0.0	270	0	938.586	405.0	5000
	K-a1	0.003	0.0	90	0	342.723	135.0	5000
	A-a1	0.003	0.01	90	300	342.723	135.0	2000
	E-d4	0.02	0.2	36	360	132.736	54.0	3000
Coil	L-l1	0.0004	0.0	90	0	605.855	324.0	5000
	L-i1	0.003	0.0	90	0	221.227	324.0	5000
	F-i7	0.003	0.01	30	100	221.227	108.0	5000
	J-j7	0.02	0.2	30	300	85.681	108.0	3000

2.4. Dependence on the solution conditions

The simulations are planned to compare the MC results with the titration data of L-PGA in aqueous solutions. The helix-to-coil transition occurs in the titration range. The practical simulations are performed for the following series of data to examine the availability of the models, and to investigate the properties of the helix–coil transition.

2.4.1. Polymer concentration dependence

The dependence of the titration behavior on the polymer concentration was investigated [15,16]. To examine the polymer concentration dependence by the MC method, the experiments of L-PGA by Nitta et al. [12] are compared with the simulated results. They obtained little dependence on polymer concentration when it is lower than salt concentration (C^p = 0.0065, 0.0132, and 0.0277 N in 0.05 M KCl), and a large dependence when polymer concentration is higher than salt concentration (C^p = 0.0065, 0.0119, 0.0191 and 0.0363 N in 0.005 M KCl) at 25° C.

It is the object to examine the polymer concentration dependence by the MC method. The cell sizes and other parameters are determined to generate the solution conditions similar to the experiments (Table 3). The difference between NaCl and KCl is ignored.

2.4.2. Ionic strength dependence

The simulation is attempted to examine the ionic strength dependence by comparing with the titration data of L-PGA by McDiarmid and Doty [17]. They presented the titration curves of 0.0004 N residues without salt and 0.003 N in 0, 0.01, 0.2 and 2.0 M $NaClO_4$ solutions at 25° C. Except for the case of 2.0 M salt solution, these titration curves can be simulated by the MC method. The C^p in the simulation is 0.0004, 0.003 or 0.02 N (Table 4). Though the large coion, ClO_4^-, was used in the experiment, the radius, 2.0 Å is adopted because the coion size scarcely affects the results.

In addition, the well-known data of L-PGA by Nagasawa and Holtzer [13] are checked as the cases of high polymer concentration. In the experiment, C^p is 0.0188 or 0.0342 N, the C^S (NaCl) range is 0.005 to 0.2 M, and the temperature is 25° C. The simulations are attempted only for the data in Fig. 1 in their paper. The cell sizes and other parameters are shown in Table 5.

2.4.3. Temperature dependence

Olander and Holtzer presented the titration curves of L-PGA at various temperatures, and represented the titration curves at 0.6° C, 25.5° C and 48° C in 0.1 M NaCl solutions. The simulations are carried out to analyze the temperature dependence of the titration curve by comparing with the experimental data. The applied C^p in the experiments was in about 0.015–0.02 N range [11]. In the MC simulation, 0.02 N is

Table 5
Parameters of the objective cell of the helical and coiled PGA for the investigation of the ionic strength dependence

Label	C^p (N)	C^s (M)	N^p	N^s	Helix		Coil		MCS	Symbol
					R (Å)	H (Å)	R (Å)	H (Å)		
I (m)	0.01875	0.005	90	24	137.089	135.0	88.491	324.0	5000	Square
II (n)	0.01875	0.02	90	96	137.089	135.0	88.491	324.0	5000	Circle
III (o)	0.03396	0.02	90	53	101.861	135.0	65.751	324.0	5000	Square
IV (p)	0.01875	0.2	54	576	137.089	81.0	88.491	194.4	2000	Circle

Comparing data are obtained by Nagasawa and Holtzer.
Symbols in the rightmost column are used in Fig. 7.

used as C^p. Cell parameters are similar to those mentioned in Section 2.2 (for helix: label 'D-d4' in Table 1, for coil: label 'H-g7' in Table 2). Then, the dielectric constant, D, and Bjerrum length, $l_B = e^2/(4\pi\varepsilon_0 Dk_B T)$, at each temperature are 87.90, 6.944 Å at 0.6° C, 78.55, 7.135 Å at 25.0° C, and 70.79, 7.350 at 48° C, respectively [18]. As a middle temperature, 25.0° C is applied instead of 25.5° C, for convenience.

3. Results and discussion

3.1. Titration profiles of the helical and coiled forms

Considerable agreements of the titration curves with the experimental data are achieved in the helical and coiled conformation models of PGA, respectively, described as follows.

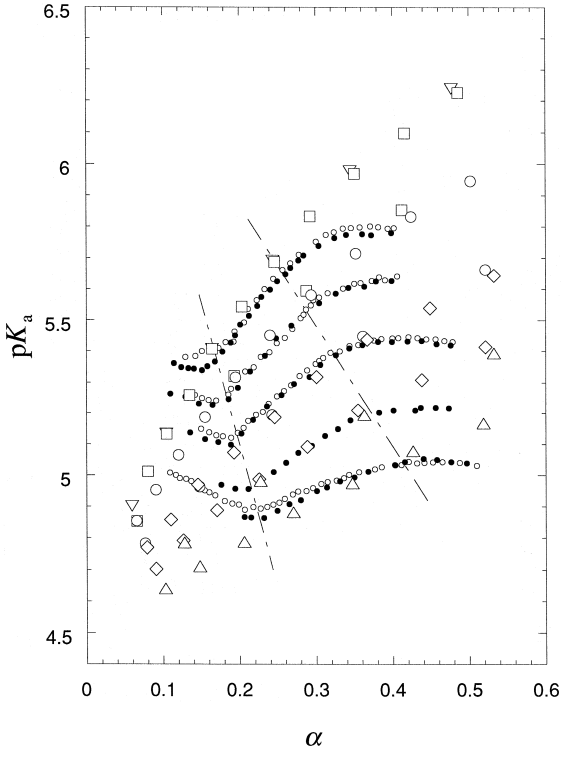

Fig. 2. Simulated titration curves of α-helical PGA in 0.01, 0.02, 0.05, 0.1 and 0.2 M salt solutions (from top to bottom). The results of the MC simulations (large symbols) are represented with the experimental data (small symbols) obtained by Muroga et al. Two small symbols represent the difference of the polymer concentration C^p (open circle: 0.001, closed circle: 0.002–0.003 N) in the experiments. See Table 1 for large symbols. The region between two chained lines means the helical portion of the peptide.

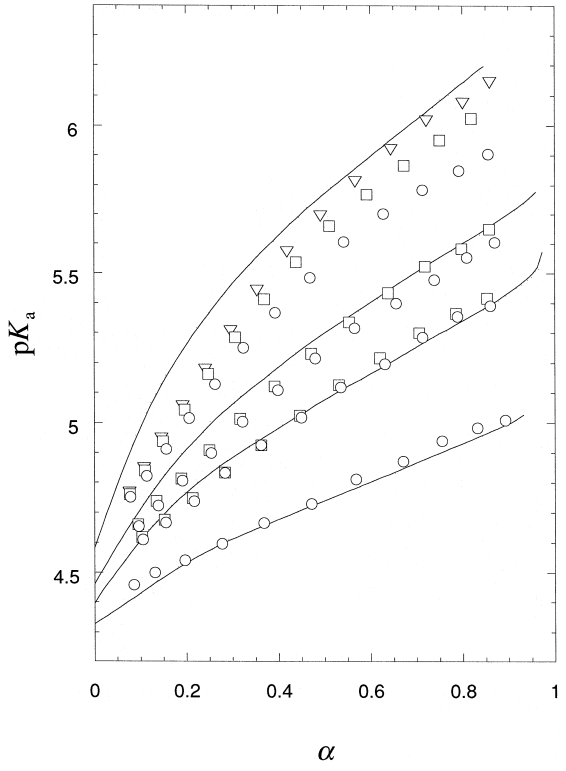

Fig. 3. Simulated titration curves of extended DL-PGA in 0.01, 0.05, 0.1 and 0.4 M salt solutions (from top to bottom). The results of the MC simulations (symbols) are represented with the experimental data (lines) obtained by Olander and Holtzer. The difference of symbol signifies the different C^p. See Table 2.

3.1.1. α-Helix

The agreement of the simulation data with the experiments is satisfied in α-helical region (Fig. 2). The pK_0 is given as 4.70 for all salt concentrations to fit the experiments. The dependence on the polyion concentration scarcely appears in the cases. It seems that the dependence on the salt concentration is slightly larger in the simulation than that of the experiment. It is probably due to the inaccuracy of the molecular model. This model is, however, suited enough to use for analysis of the transition.

3.1.2. Extended coil

The comparisons of the simulation curves with experiments are presented in Fig. 3, when the pK_0 is

given as 4.68 for all salt concentrations. The simulation data for the extended coil sufficiently agree with the experiments. The relatively small deviations in low α range are probably ascribed to the effect of polymer flexibility, similar to the case of poly(acrylic acid) [19]. In addition, the dependence on the polymer concentration is observed in the case of lower salt concentrations. The C^p dependence is significant at the lowest salt concentration ($C^S = 0.01$ M). The agreement of the simulation is fairly good at $C^p = 0.005$ N. Nevertheless, its appropriateness cannot be judged because the precise C^p value is unknown.

Furthermore, a remarkable dependence of the titration curve on θ^p is found in the extended coil model (data not shown). The curve of L-PGA ($\theta^p = 180°$) goes below that of DL-PGA ($\theta^p = 80°$). Similar divergence was also observed between DL-PGA and the coil portion of L-PGA in the experiments [11].

3.2. Helix–coil transition of L-PGA

The results of the fitting of the helical and coiled forms and the characteristics of the helix–coil transition are presented and discussed below. The energetic properties are interpreted for the helix–coil transition of L-PGA.

3.2.1. Polymer concentration dependence

The results of the simulations are shown with the experimental ones in Fig. 4. The tendencies of the polymer concentration dependence are essentially reproduced by the MC simulations. However, considerable deviations appear in cases of higher polymer concentration for the coiled form. The curves in the helix region are well fitted by the simulations in both cases. The common pK_0 value is 4.66 in comparison with the experiments.

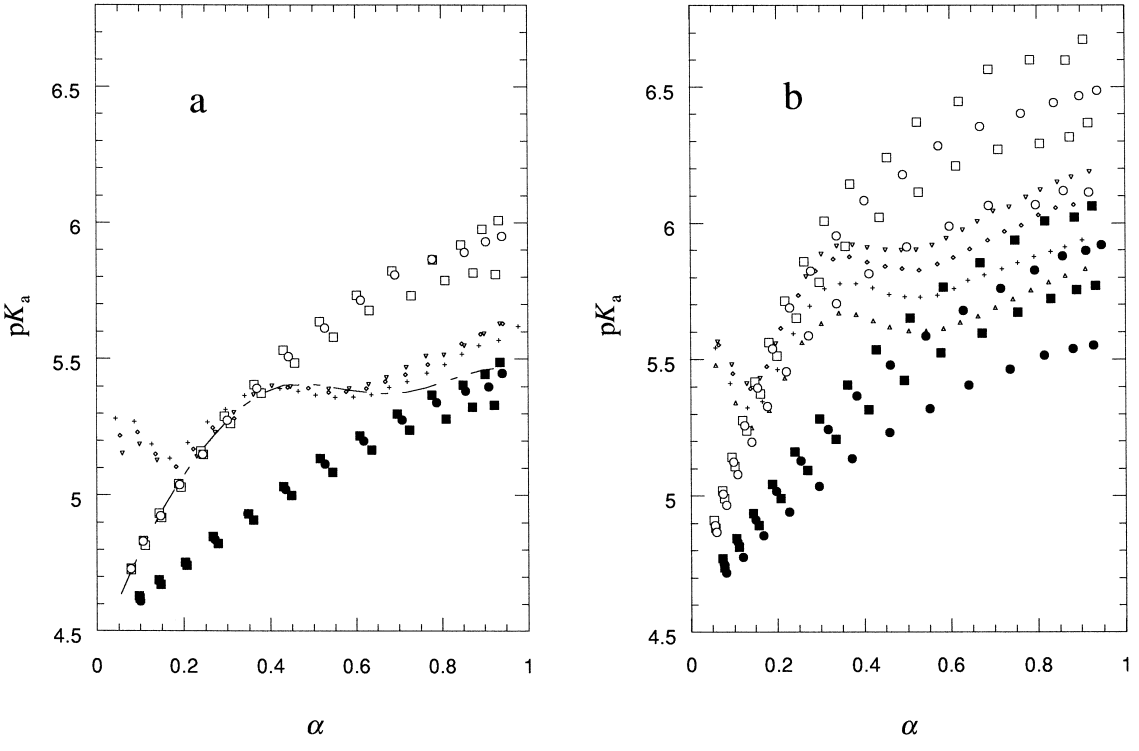

Fig. 4. The calculated titration curves of L-PGA (large symbols; open symbols: helix, closed symbols: coil) with the experimental data (small symbols) obtained by Nitta et al. See Table 3 for the parameters in the simulations. (a) polymer concentration ($C^p = 0.0065$, 0.0132, and 0.0277 N from top to bottom) is lower than salt concentration (0.05 M KCl). Dashed curve denotes the calculated helix–coil transition in the most dilute polymer case ($s_0 = 1.51$, and $\sigma = 0.0028$). (b) polymer concentration ($C^p = 0.0065$, 0.0119, 0.0191 and 0.0363 N from top to bottom) is higher than salt concentration (0.005 M KCl).

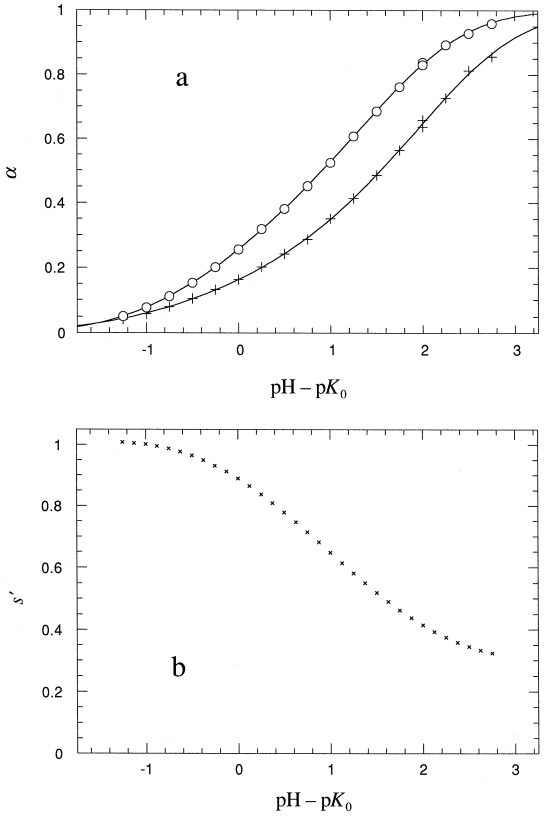

Fig. 5. The example of the calculation of the helix–coil transition curve in 0.01 M salt solution obtained by the MC simulations. (a) The (pH–pK_0) vs. α_h and α_c curves. Plus: helix (label 'A-a1' in Table 4), and circle: extended coil (label 'F-i7'). The lines signify the fitting curves. (b) The (pH–pK_0) vs. calculated s' curve evaluated from the data shown in (a).

The dependence of the titration curve on the polymer concentration is small in cases of high salt and low polymer concentration. This fact is reproduced by the MC simulations (Fig. 4a). However, the polymer concentration dependence is larger than that in the experiments. In addition, the calculated curves for the coil are slightly lower than the experimental curves. The fitting to the helix–coil transition is attempted only for the most dilute solution ('r-1' in Table 3) shown as a dashed curve in Fig. 4a.

The downward deviation of the curves for the coil becomes larger in cases of low salt and high polymer concentration (Fig. 4b). The departure becomes larger as the polymer concentration increases. On the other hand, the helix curve agrees well at a given pK_0 value in each condition. Then, the evaluation of the transition parameter is difficult in these cases.

3.2.2. Ionic strength dependence

The MC simulations are carried out for the titration process of PGA in helix and extended coil form, respectively. The experiments at the low polymer concentration by McDiarmid and Doty are well reproduced by the simulations. In Fig. 5a, the degree

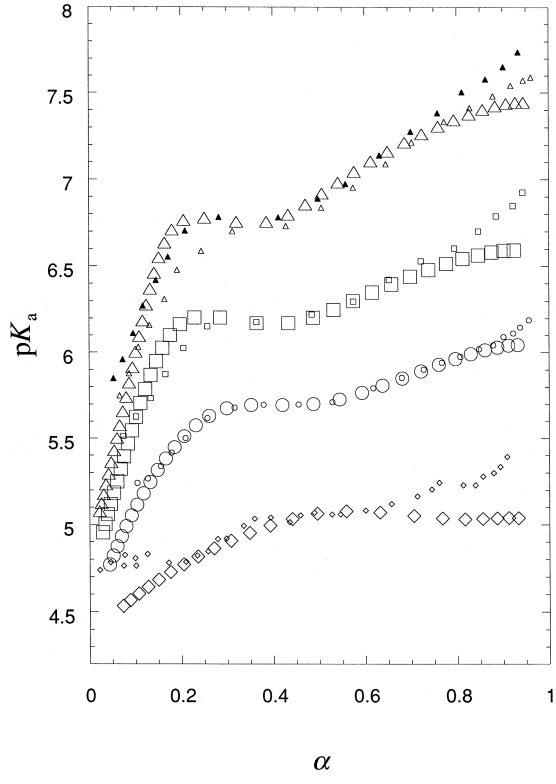

Fig. 6. The calculated titration curves of L-PGA (large symbols) with the experimental data (small symbols) obtained by McDiarmid and Doty. The experimental data are in (closed and open triangle) $C^p = 0.0004$ N, $C^s = 0.0$ M; (square) $C^p = 0.003$ N, $C^s = 0.0$ M; (circle) $C^p = 0.003$ N, $C^s = 0.01$ M; and (diamond) $C^p = 0.003$ N, $C^s = 0.2$ M, from top to bottom. See Table 4 for cell parameters and Table 6 for fitting parameters.

Table 6
Parameters for the helix–coil transition obtained by the fitting to the experimental data at different ionic strengths by McDiarmid and Doty

Label helix → coil	C^p (N)	C^s (M)	s_0	$\Delta g^\circ_{hc} \times 10^{21}$ (J/residue)	Δg°_{hc} (cal/mol)	σ	Symbol
K-ka → L-l1	0.0004	0.0	1.86	2.55	368	0.0028	Triangle
K-a1 → L-i1	0.003	0.0	1.66	2.09	300	0.0028	Square
A-a1 → F-i7	0.003	0.01	1.44	1.50	216	0.0028	Circle
E-d4 → J-j7	0.02	0.2	1.44	1.50	216	0.0028	Diamond

Labels in the leftmost column are used in Table 4.
Symbols in the rightmost column are used in Fig. 6.

of ionization of each conformation is represented as a function of pH−pK_0. The fitting is enough to evaluate the s' values accurately (Fig. 5b).

Using the fitting parameters, the transition curve is calculated for each titration data as presented in Fig. 6. The common pK_0 value is 4.68 in comparison with the experiments. The agreements are almost satisfied in whole data even in the nosalt cases. The deviations appear in high α range. Especially, the coil portion in 0.2 M salt case is significantly deviated from the experiment, although the reason is unclear. However, the experimental errors generally increase in the region. In the calculations, the value of σ is fixed to 0.0028 in all cases. Though the larger values may be preferable to fit the data in the no salt cases, the evaluation of the precise values is difficult. The parameters for the transition are within the suitable range (Table 6). The slight dependence of s_0 on the ionic strength is observed [13].

Contrary to the above results, the curves at the high polymer concentration by Nagasawa and Holtzer cannot be sufficiently reproduced (Fig. 7). Here, the common pK_0 value, 4.68, is adopted in comparison with the experiments. The simulated curves for the helix agree well with the experimental data (region B). Those for the coil deviate largely from the experiments (region D). The helix–coil transition parameters cannot be evaluated in these cases.

3.2.3. Temperature dependence

The temperature dependence does not appear in the separated simulations of the helix and coil form (data not shown). Therefore, the fitting of the curves is executed using the common parameters for the data at three temperatures. By giving the appropriate values for s_0 and σ at each temperature, the transition curves are represented in Fig. 8. The common pK_0 is set to be 4.80 in this case. The agreement is satisfactory, and the parameters are reasonable. The small deviation in low α range may be the appearance of the limitations of our simple models and hypothesis (Eq. (11)).

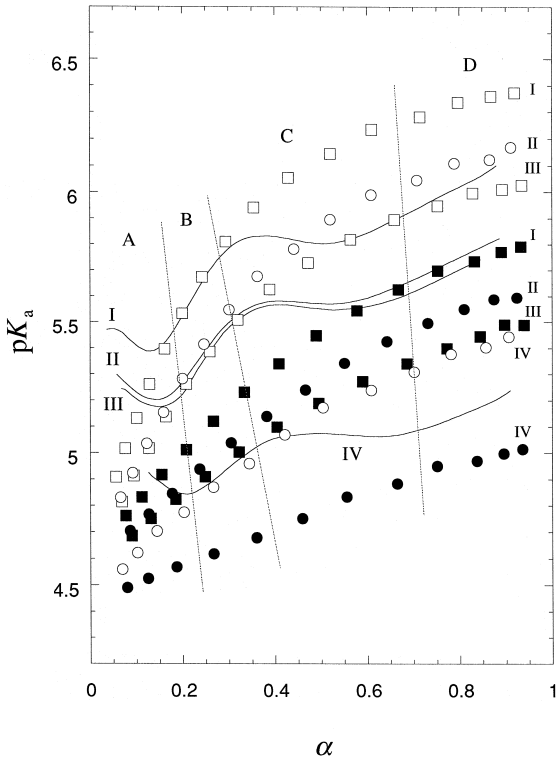

Fig. 7. The simulated data of L-PGA helix and coil (symbols) with the experimental data (lines) obtained by Nagasawa and Holtzer. Open symbols: helix, closed symbols: coil. I, $C^p = 0.0188$ N, $C^s = 0.005$ M; II, $C^p = 0.0188$ N, $C^s = 0.02$ M; III, $C^p = 0.0342$ N, $C^s = 0.02$ M; and IV, $C^p = 0.0188$ N, $C^s = 0.2$ M, from top to bottom, respectively. See Table 5. Vertical dotted lines divide the region in the helix to coil transition processes (A to D).

A slightly larger pK_0 value and a smaller σ value are used than the above calculations for the fitting to the data. The divergence is considerably small taking account of the independence of the experiments by the distinct research groups.

The temperature dependence of the parameters is represented by Arrhenius plot in Fig. 9. The linear dependence of each parameter on $1/T$ is represented. The values of Δg°_{hc} are 224, 164, and 116 cal/mol at 0.6° C, 25° C and 48° C, respectively. It means that the fitting using the MC results is successfully achieved.

3.3. Remaining problems

3.3.1. On the ambiguities of the pK_0 value and the molecular model

In the simulations, the difference of the given pK_0 value between helix and coil conformations is within the experimental error. Furthermore, nearly the same pK_0 values (4.66–4.70) are applied in the helix–coil simulations with one exception (temperature dependence case). This indicates a wide applicability of this model. Nevertheless, Nozaki and Tanford had obtained the intrinsic value, 4.50 ± 0.06 for glutamyl carboxyl group [20]. Rinaudo and Domard evaluated the mean value $pK_0 = 4.40$ for glutamic acid oligomer [21]. The pK_0 values used in the MC studies are slightly higher than that in the other works, although the definition of pK_0 in the MC work is not rigorously identical to the experimental one. There is a possibility that the increases in pK_a with α is slightly small in the simulation, and that the high pK_0 value is necessary for fitting to the data. Indeed, if larger size of mobile ion (e.g., $\sigma_m =$ 2.5 Å) is adopted, smaller pK_0 value becomes preferable for fitting the data. Several data, however, are poorly fitted at the condition. There are some ambiguities. Here, the above-mentioned molecular models and the mobile ions of radius 2.0 Å are chosen to interpret the possibly various data within less dispersion of pK_0 value.

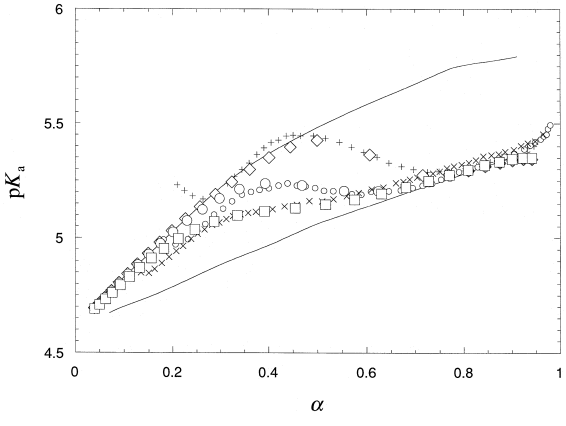

Fig. 8. The calculated titration curves at three temperatures of L-PGA (large symbols) in 0.1 M salt with the experimental data (small symbols) obtained by Olander and Holtzer. Large symbols: ◇: 0.6° C, ○: 25° C, □: 48° C. Small symbols: +: 0.6° C, ○: 25.5° C, ×: 48° C. Lines signify the simulation data for the complete helical (upper) and coiled (lower) PGA at all temperatures.

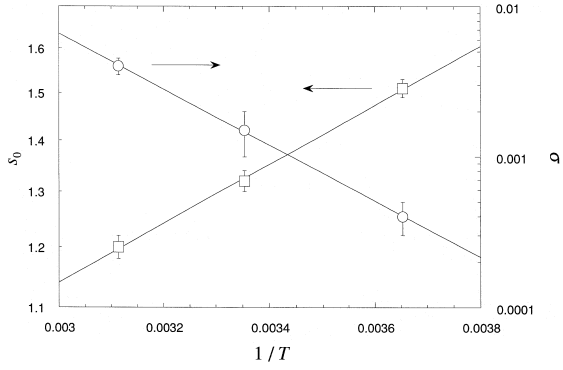

Fig. 9. The Arrhenius plot of the transition parameters, s_0 (□, left axis) and σ (○, right axis) used in Fig. 8. The error bars are added based on the presumptive values. The lines signify the linear fitting. Obtained relations are represented with linear equations, those are, $\ln s_0 = -1.1503 + 427.14/T$ and $\ln\sigma = 7.8121 - 4276.7/T$.

3.3.2. On the polymer concentration dependence

The simulation can reproduce the dependence of the titration curve on the polymer concentration qualitatively. However, appreciable deviations are observed for the extended coil form in the cases of higher polymer concentration. The polymer concentration dependence of the present MC work is larger than that of the Poisson–Boltzmann (PB) equation calculated by Nitta et al. [12] by assuming unrealistic large radius of the polyion. This is possibly due to some oversimplification existing in the present molecular model, compared with the actual confor-

mation of the polyion. In high α range, the dimensions of the polymer affect the titration curve as shown in the simulations of CMC [9]. It is difficult that most of the experimental data are exactly simulated by a unique molecular model. In the simulation, relatively large amounts of the counterions probably accumulates around the polyion rod especially at high polymer concentration within thin cylindrical cell, compared with the results of the PB equation. It seems that the restriction of our simple interaction model appears in cases of high polymer concentration. More investigation is required on this point.

4. Conclusion

The titration curves of the helical form and extended coil form of PGA are reproduced by the simulation separately. The agreement of the dependence on the salt concentration is fulfilled. The dependence on the polymer concentration appears in the simulations for the coiled form in the cases of high polymer concentration.

The helix–coil transition curves of L-PGA are also represented using the Zimm–Bragg theory. The polymer concentration dependence is essentially reproduced. However, appreciable departures from the experiments appear in the concentrated polymer solutions. The dependence on the ionic strength and on the temperature is reproduced with the appropriate transition parameters, unless the polymer concentration is so high. In a few cases, larger mobile ion radius is preferable to fit the experimental data. Although several ambiguities remain, the reproduction of the experiments is considerably achieved.

Acknowledgements

The author is grateful to Professor A. Minakata for valuable suggestions and critical reading of the manuscript. The practical calculations of the MC simulation were executed on the vector processor in the computational center of Nagoya University and in the information processing center of Hamamatsu University School of Medicine.

References

[1] P. Doty, A. Wada, J.T. Yang, E.R. Blout, J. Polym. Sci. 23 (1957) 851.
[2] B.H. Zimm, S.A. Rice, Mol. Phys. 3 (1960) 391.
[3] D. Poland, H.A. Scheraga, Theory of Helix–Coil Transitions in Biopolymers, Academic Press, New York, 1970.
[4] H. Qian, J.C. Schellman, J. Phys. Chem. 96 (1992) 3987.
[5] A. Holtzer, J. Am. Chem. Soc. 116 (1994) 10837.
[6] A. Chakrabartty, R.L. Baldwin, Adv. Protein Chem. 46 (1995) 141.
[7] T. Nishio, Biophys. Chem. 49 (1994) 201.
[8] B.H. Zimm, J.K. Bragg, J. Chem. Phys. 31 (1959) 526.
[9] T. Nishio, Biophys. Chem. 57 (1996) 261.
[10] Y. Muroga, K. Suzuki, Y. Kawaguchi, M. Nagasawa, Biopolymers 11 (1972) 137.
[11] D.S. Olander, A. Holtzer, J. Am. Chem. Soc. 90 (1968) 4549.
[12] K. Nitta, M. Yoneyama, N. Ohno, Biophys. Chem. 3 (1975) 323.
[13] M. Nagasawa, A. Holtzer, J. Am. Chem. Soc. 86 (1964) 538.
[14] J. Applequist, J. Chem. Phys. 38 (1963) 934.
[15] H. Maeda, F. Oosawa, J. Phys. Chem. 76 (1972) 3445.
[16] K. Nitta, S. Sugai, J. Phys. Chem. 78 (1974) 1189.
[17] R. McDiarmid, P. Doty, J. Phys. Chem. 70 (1966) 2620.
[18] J. Wyman Jr., E.N. Ingalls, J. Am. Chem. Soc. 60 (1938) 1182.
[19] T. Nishio, A. Minakata, Rep. Progr. Polym. Phys. Jpn. 40 (1997) in press.
[20] Y. Nozaki, C. Tanford, J. Biol. Chem. 242 (1967) 4731.
[21] M. Rinaudo, A. Domard, Biopolymers 12 (1973) 2211.